Role of the 2D Surface State Continuum and Projected Band Gap in Charge Transfer in Front of a Cu(111) Surface

T. Hecht and H. Winter
Institut für Physik, Humboldt-Universität zu Berlin, Invalidenstraße 110, D-10115 Berlin, Germany

A. G. Borisov and J. P. Gauyacq
Laboratoire des Collisions Atomiques et Moléculaires, Unité Mixte de Recherche CNRS-Université Paris Sud UMR8625, bâtiment 351, 91405 Orsay Cedex, France

A. K. Kazansky
Institute of Physics, St. Petersburg University, 198904 St. Petersburg, Russia
(Received 2 November 1999)

Electron capture by Li^+ and H projectiles in grazing scattering from Cu(111) and Cu(110) surfaces is studied experimentally and theoretically. Whereas data for Cu(110) can be described by established theoretical methods treating resonant charge transfer with a free-electron metal, data for Cu(111) show pronounced deviations from this approach. We interpret our observations by the effect of the projected L-band gap of the Cu(111) surface. In particular, the quantum states of reduced dimension (2D surface state continuum) play a dominant role in electron transfer.

PACS numbers: 79.20.Rf, 34.70.+e, 68.35.Bs, 73.20.At

Charge transfer processes between atomic species and solid surfaces are of paramount importance for a variety of gas-surface interaction phenomena, such as scattering, sputtering, adsorption, and molecular dissociation, as well as for surface analysis tools. As a consequence, many experimental and theoretical studies have been devoted to this subject (see, e.g., reviews [1,2]). The one-electron energy-conserving transition corresponding to the tunneling between electronic levels of the projectile and metal surface, the so called *resonant charge transfer* (RCT) process, is particularly well understood for free-electron (jellium) metals. Nowadays, theoretical methods are available that allow for parameter-free quantitative descriptions of RCT in this case [3–6].

On the other hand, the important question of an influence of the band structure of the target metal on charge transfer processes has hardly been explored so far, except for a few perturbative treatments (see, e.g., Ref. [7]). Progress achieved in the understanding of electron transfer for realistic surfaces would be of immediate relevance for the basic understanding and technological applications of gas-surface interactions. The (111) surfaces of noble metals are particularly well suited for this kind of investigation. The quasifree sp-electron band exhibits a projected band gap (L gap) which extends from -5.83 to -0.69 eV with respect to the vacuum in the Cu(111) case [8]. Within this energy range, electrons cannot penetrate into the crystal along the surface normal. This leads to the possibility of quantized states for the motion normal to the surface. Associated with propagating states in the directions parallel to the surface, they form two-dimensional (2D) state continua (surface and image state continua) that are localized in (or close to) the surface region. For Cu(111) the bottom of the surface state continuum is located at $E_{SS} = -5.33$ eV with respect to the vacuum [8]. The surface and image potential states, localized within the projected band gap, are presently the subject of intense theoretical and experimental research, in particular, involving two-photon-photoemission spectroscopy with femtosecond lasers. This interest is caused by the role played by these states in electron dynamics at clean and adsorbate covered metal surfaces, and, correspondingly, in surface photochemistry [9–12].

Recent theoretical studies of the RCT process between atomic projectiles and a Cu(111) surface revealed several interesting features [13]. (i) For projectile states of energies within the projected band gap, the resonant charge transfer rates are, as a rule, strongly reduced. This blocking is due to the fact that electron tunneling along the surface normal, which is the preferential direction, is made impossible by the projected band gap. (ii) The band gap effect depends on the interaction time. It disappears for large perpendicular velocities of the projectile. These findings are supported by recent experiments [14–16].

In this Letter, we report on a joint experimental and theoretical effort in order to elucidate the role played by the 2D surface state continuum in the RCT process. We demonstrate that experiments, performed in grazing collision geometry, are particularly well suited to study this problem. As representative examples, we discuss the H^- ion formation and Li^+ neutralization at Cu(111) and Cu(110) surfaces. The Cu(110) surface has no projected band gap in the direction of the surface normal and, correspondingly, no surface state at the Γ point. We use it as a reference against which to test for band gap effects.

In the experiments, H^+ and Li^+ ions with velocities ranging from 0.05 to 1 a.u. are scattered under a grazing

angle of incidence $\Phi_{in} \approx 1°$ from atomically flat and clean Cu(111) and Cu(110) surfaces. The surfaces were prepared by cycles of grazing sputtering with 25 keV Ar^+ ions and subsequent annealing for about 10 min at a temperature of about 550 °C. The base pressure in the differentially pumped UHV-scattering chamber was some 10^{-11} mbar. Charge fractions are obtained by dispersing the well defined scattered beams with electric field plates. The projectiles are detected by a channeltron, its entrance aperture being covered by a thin carbon foil in order to obtain an equal response of the detector to projectiles in different charge states. The work function of 4.95 ± 0.03 eV for Cu(111) and 4.49 ± 0.03 eV for Cu(110) target surfaces was measured *in situ* by photoemission.

Our theoretical treatment of the RCT process is based on the wave-packet propagation (WPP) method presented in detail elsewhere [13]. Briefly, this method consists of the direct solution of the time-dependent Schrödinger equation for the electron active in charge transfer. Model potentials are used to describe electron interaction with projectile core [13]. In the Li case, the Li^+ core image is also included. Two descriptions for the metal surface are used. Within the jellium model [17] the electron-metal interaction potential is constant in the bulk and smoothly joins the image potential tail in vacuum. The Cu(111) surface is described with a potential given by Chulkov *et al.* [8]. It takes into account the periodicity of the crystal in the direction of the surface normal but assumes free motion in the directions parallel to the surface. It reproduces the gross features of the Cu(111) surface: projected band gap, surface state, and image states.

For grazing scattering the collision velocity component perpendicular to the surface ($v_\perp$) is small (some 10^{-2} a.u.). Then we deduce from the WPP approach that the evolution of the population of the projectile states can be described by a rate equation (RE). On the other hand, the velocity component parallel to the surface is large, so that one has to take into account the Galilei transformation from the projectile to the surface frames.

Within the RE approach, the evolution of the projectile population along the trajectory is described in terms of electron capture and loss rates (Γ^c and Γ^l) [6,18]. These rates depend on the projectile-surface distance Z, energy $E_a(Z)$, and width $\Gamma(Z)$ of the projectile level in front of the surface. Parallel velocity effects are incorporated via the shifted Fermi sphere model [1]. For the 3D free-electron continuum (jellium metal target), the capture and loss rates can be derived in a spherical coordinate basis (the z axis is along the surface normal and goes through the projectile center) [6,18,19]:

$$\begin{Bmatrix} \Gamma^c(Z) \\ \Gamma^l(Z) \end{Bmatrix} = \Gamma(Z) \begin{Bmatrix} g^c \\ g^l \end{Bmatrix} \int_0^\pi |\sigma(\theta, Z)|^2 \sin\theta \, d\theta \times \int_0^{2\pi} d\varphi \begin{Bmatrix} f[(\vec{k} + \vec{v}_\parallel)^2/2] \\ 1 - f[(\vec{k} + \vec{v}_\parallel)^2/2] \end{Bmatrix}. \quad (1)$$

The metal-state electron wave vector $\vec{k} = (k, \theta, \varphi)$ satisfies the resonance condition $k = \sqrt{2(E_a(Z) - U)}$, where U is the energy of the bottom of the conduction band. g^c and g^l are spin statistical factors. $|\sigma(\theta, Z)|^2$ is the normalized angular distribution of the transition probability. $f[(\vec{k} + \vec{v}_\parallel)^2/2]$ is the Fermi-Dirac distribution, modified by the Galilei transformation.

The interpretation of Eq. (1) is straightforward: the capture (loss) rate depends on the number of occupied (empty) metal states in resonance with the atomic state. The phase space is weighted by the transition probability which is strongly peaked in the direction of the surface normal (the "easiest" direction for electron transfer). For H^- ions, this results in $\Gamma^c \ll \Gamma^l$, leading to small H^- yields as was observed for an Al(111) surface [6,19]. All quantities in Eq. (1) can be derived from WPP or other methods [6,18]. The results for H^- formation (jellium model) are displayed in Figs. 1(a) and 1(b). Negative ion fractions of a few 10^{-3} are predicted for jellium-Cu surfaces. Owing to the work-function difference, the jellium model predicts that less H^- ions are formed at Cu(111) than at Cu(110). The width of the kinematic resonance structure for the H^- yields is related to the diameter of the Fermi sphere ($2k_F$), $k_F = 0.72$ a.u. in the present case.

The situation is different for the model Cu(111) surface. From the WPP study we obtain that the coupling of the projectile states with the 2D surface state continuum is 1 order of magnitude stronger than with the 3D bulk continuum. (The contribution of the 2D image state continuum is negligible.) Within our Cu(111) model, the surface state continuum corresponds to electrons moving freely in the plane parallel to the surface with an energy $E = E_{SS} + k_\parallel^2/2$. $\vec{k}_\parallel = (k_\parallel \cos\varphi, k_\parallel \sin\varphi)$ is the 2D electron wave vector. For the capture and loss rates in the 2D case one obtains [20]

$$\begin{Bmatrix} \Gamma^c(Z) \\ \Gamma^l(Z) \end{Bmatrix} = \Gamma(Z) \begin{Bmatrix} g^c \\ g^l \end{Bmatrix} \frac{1}{2\pi} \times \int_0^{2\pi} d\varphi \begin{Bmatrix} f[(\vec{k}_\parallel + \vec{v}_\parallel)^2/2] \\ 1 - f[(\vec{k}_\parallel + \vec{v}_\parallel)^2/2] \end{Bmatrix}, \quad (2)$$

where $k_\parallel$ is given by the resonance condition $k_\parallel = \sqrt{2(E_a(Z) - E_{SS})}$.

Parallel velocity assisted charge transfer in 2D clearly differs from that in 3D. The Fermi sphere is replaced by a Fermi disk. The only remaining angular variable is the azimuth φ so that the phase space is not weighted anymore by the transition probability [20,21]. In the case of the H^- ion, this leads to an increase of the capture rate relative to the loss rate. In addition, the Fermi level for Cu(111) is close to the bottom of the surface state continuum: $E_F - E_{SS} = 0.38$ eV. Thus $k_F = 0.17$ a.u. is small, and the width of the kinematic resonance in the H^- fraction is rather narrow. Calculated H^- fractions for the jellium model (3D continuum) and model Cu(111) (2D

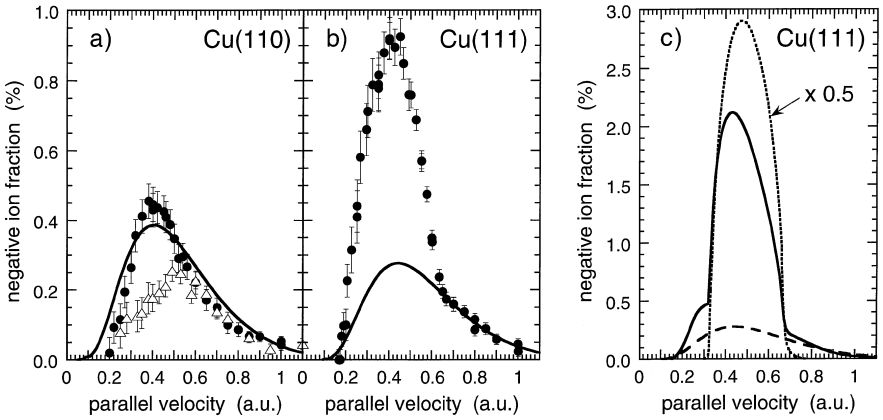

FIG. 1. H^- charge fraction for hydrogen scattered from Cu surfaces as a function of the collision velocity parallel to the surface. The perpendicular velocity is kept fixed at 0.02 a.u. (a) Cu(110) surface. Solid line: Theory (jellium model, 3D); dots and triangles: experimental data taken for the scattering close to the $\langle 001 \rangle$ and $\langle \bar{1}10 \rangle$ directions. (b) Cu(111) surface. Solid line: Theory (jellium model, 3D); dots: experiment. (c) Theoretical results for the Cu(111) surface. Dashed line: Jellium model (3D); dotted line: model Cu(111) (2D band only); solid line: model Cu(111) including multielectron effects and electron capture from 2D and 3D bands (see text).

continuum) are represented by dashed and dotted lines in Fig. 1(c). The negative ion yields obtained in the 2D case are much larger (up to 6%) and exhibit a more narrow parallel velocity resonance (note the multiplicative factor on the 2D results).

Experimental H^- fractions for scattering from Cu(110) and Cu(111) surfaces are shown in Figs. 1(a) and 1(b). The general trends predicted by calculation can be seen in the experimental data. In particular, despite the work function difference, clearly more negative ions are formed at the Cu(111) surface. The narrow kinematic resonance structure is superimposed on an apparently broader one, ascribed to contributions of the 3D bulk continuum. While the jellium calculations describe experimental data for Cu(110) reasonably well, they fail for the Cu(111) data. Interestingly, at large parallel velocities, when the electronic structure of the target is smeared out in the projectile frame, the difference between Cu(111) and Cu(110) disappears and jellium calculations are close to experimental data (see also Fig. 2). In passing we note that an azimuthal dependence of the H^- yields observed for Cu(110) presumably also indicates a band structure effect. So, the applicability of the jellium model should not be overestimated even in this case, when the band gap blocking effect is absent. No azimuthal dependence is observed for Cu(111).

While correctly reproducing the main trends in the experimental H^- yields, the theoretical results for the model Cu(111) overestimate the negative ion fractions by about a factor of 6. Note that the model description of the Cu(111) surface used here neglects the band structure in the direction parallel to the surface. Thus, only gross features of the experimental data can be reproduced by our calculations. One can stress that the smallness of the H^- formation probability makes it quite sensitive to theoretical approximations. A detailed quantitative account could be reached only via inclusion of the complete (3D) band structure of copper. This formidable task was not attempted here.

There are two other possible reasons for this discrepancy. First, electron transfer from/to the 3D bulk continuum can contribute, although in a rather small manner. Second, additional electron loss by the projectile can be induced by electron-electron (e^--e^-) interactions. The latter has been estimated by introducing a complex absorbing potential inside the metal in the WPP calculation in analogy to low-energy electron diffraction

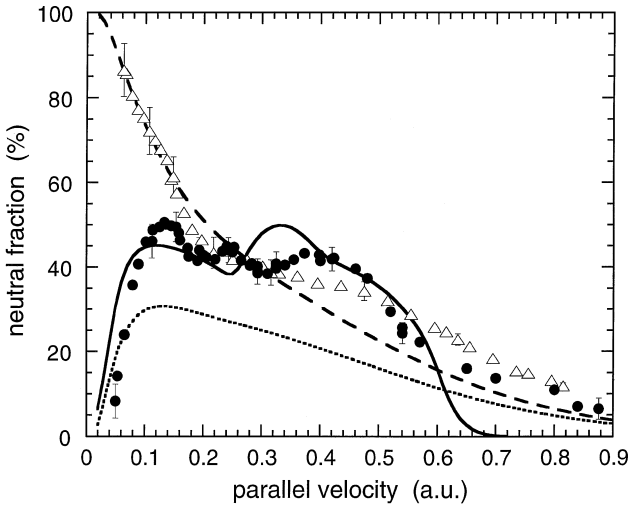

FIG. 2. Neutralization of Li^+ ions scattered at grazing angle (1.3°) from Cu surfaces as a function of the collision velocity parallel to the surface. Typical error bars are shown. Triangles: experimental data for Cu(110) surface taken for the scattering close to the $\langle 001 \rangle$ direction. Full dots: Experimental data for the Cu(111) surface. Lines represent theoretical results. Dashed line: Cu(110) (jellium model, 3D); dotted line: Cu(111) (jellium model, 3D); solid line: model Cu(111) including multielectron effects and capture from the 2D band.

(LEED) calculations [22]. This potential depends on the energy of the projectile electron according to Fermi-liquid theory: $V = -iV_0(E_a + v_\parallel^2/2 - E_F)^2$. The parameter $V_0 = 0.012\ \mathrm{eV}^{-1}$ was obtained from time resolved two-photon-photoemission experiments [23]. The inclusion of e^--e^- interactions substantially increases the electron losses in the Cu(111) case. It is worth mentioning that usually multielectron processes are weaker than the one-electron RCT and, indeed, we find no effect for the jellium surface. However, the blocking of the RCT by the projected band gap increases the relative importance of the multielectron processes. In Fig. 1(c), the solid line represents the results of the improved theoretical treatment, taking into account electron losses due to e^--e^- interactions, as well as the contribution of the 3D bulk continuum [24]. The agreement with the experimental data is improved. The maximum negative ion yield is reduced to less than 2% owing to an increased electron loss rate. Inclusion of the 3D continuum contribution leads to good agreement for large $v_\parallel$, where it dominates.

As a second example, theoretical and experimental results for the neutralization of Li^+ ions at Cu(111) and Cu(110) surfaces are presented in Fig. 2. The different shapes of parallel velocity dependence of the neutral fractions for the two surfaces can simply be related to the 0.5 eV difference in the work functions as illustrated by jellium model calculations (see also Ref. [18]). In accordance with results for H^-, the jellium model reproduces the experimental data for the Cu(110) surface, but not for Cu(111). At variance, the calculations for the model Cu(111) surface closely correspond to the experimental data. We find that the structures in the velocity dependence of the neutral fractions arise from the superposition of the Li($2s$) and Li($2p$) populations, which exhibit narrow resonant structures at different velocities. The theoretical treatment predicts a considerable excited state formation for Cu(111) in the range of parallel velocities 0.2–0.6 a.u., much larger than found for a free-electron metal [18,19]. This is again a consequence of the fact that electrons are captured from a 2D continuum. We find that the effect of the e^--e^- interactions is rather limited here. The underestimation of the neutral fractions at large velocities is attributed to the neglect of the 3D bulk continuum contribution in these calculations.

In conclusion, we have reported on a joint experimental and theoretical study on the RCT process in grazing collisions at Cu(111) and Cu(110) surfaces. We find clear evidence for a strong electronic band structure effect for a Cu(111) target, while the Cu(110) target can reasonably well be represented within the free-electron model. In particular, we have demonstrated that the charge transfer is dominated by the 2D continuum of the surface state in Cu(111). In other words, owing to the L gap that prevents electron penetration along the surface normal, the part of the system, which is effective in the electron transfer, is confined to the surface region. Besides the consequences on collisional processes illustrated here, the strong blocking of the RCT and the dominance of the 2D continuum should influence a variety of surface processes involving an electron transfer as an intermediate step.

Fruitful discussions with Professor E. V. Chulkov and Professor P. M. Echenique and assistance from K. Maas, T. Bernhard, S. Lederer, and R. A. Noack in the preparation and running of experiments are gratefully acknowledged. This work is supported by the Deutsche Forschungsgemeinschaft under Contract No. Wi 1336 and by the Franco-German PROCOPE-programme of DAAD/APAPE.

[1] R. Brako and D. M. Newns, Rep. Prog. Phys. **52**, 655 (1989).
[2] *Low Energy Ion-Surface Interactions*, edited by J. W. Rabalais (Wiley, New York, 1994).
[3] P. Nordlander and J. C. Tully, Phys. Rev. Lett. **61**, 990 (1988).
[4] J. Merino, N. Lorente, P. Pou, and F. Flores, Phys. Rev. B **54**, 10 959 (1996).
[5] S. A. Deutscher, X. Yang, and J. Burgdörfer, Phys. Rev. A **55**, 466 (1997).
[6] A. G. Borisov, D. Teillet-Billy, and J. P. Gauyacq, Phys. Rev. Lett. **68**, 2842 (1992).
[7] S. I. Easa and A. Modinos, Surf. Sci. **183**, 531 (1987).
[8] E. V. Chulkov, V. M. Silkin, and P. M. Echenique, Surf. Sci. **437**, 330 (1999).
[9] H. Petek and S. Ogawa, Prog. Surf. Sci. **56**, 239 (1997).
[10] E. V. Chulkov, I. Sarría, V. M. Silkin, J. M. Pitarke, and P. M. Echenique, Phys. Rev. Lett. **80**, 4947 (1998).
[11] A. Hotzel, K. Ishioka, M. Wolf, and G. Ertl, Chem. Phys. Lett. **285**, 271 (1998).
[12] K. Nagesha and L. Sanche, Phys. Rev. Lett. **81**, 5892 (1998).
[13] A. G. Borisov, A. K. Kazansky, and J. P. Gauyacq, Phys. Rev. B **59**, 10 935 (1999); Surf. Sci. **430**, 165 (1999).
[14] M. Bauer, S. Pawlik, and M. Aeschlimann, Phys. Rev. B **55**, 10 040 (1997).
[15] S. Ogawa, H. Nagano, and H. Petek, Phys. Rev. Lett. **82**, 1931 (1999).
[16] L. Guillemot and V. Esaulov, Phys. Rev. Lett. **82**, 4552 (1999).
[17] P. J. Jennings, P. O. Jones, and M. Weinert, Phys. Rev. B **37**, 3113 (1988).
[18] A. G. Borisov, D. Teillet-Billy, J. P. Gauyacq, H. Winter, and G. Dierkes, Phys. Rev. B **54**, 17 166 (1996).
[19] H. Winter, Comments At. Mol. Phys. **26**, 287 (1991).
[20] A. G. Borisov and H. Winter, Z. Phys. D **37**, 263 (1996).
[21] Q. Yan, J. Burgdörfer, and F. W. Meyer, Phys. Rev. B **56**, 1589 (1997).
[22] M. A. Van Hove, W. H. Weinberg, and C. M. Chan, *Low Energy Electron Diffraction* (Springer-Verlag, Berlin, 1986).
[23] T. Hertel, E. Knoesel, M. Wolf, and G. Ertl, Phys. Rev. Lett. **76**, 535 (1996).
[24] A. G. Borisov and J. P. Gauyacq (to be published).